

Accepted Manuscript

Discovery and structure-activity relationships study of thieno[2,3-*b*]pyridine analogues as hepatic gluconeogenesis inhibitors

Fei Ma, Jian Liu, Tingting Zhou, Min Lei, Jing Chen, Xiachang Wang, Yinan Zhang, Xu Shen, Lihong Hu



PII: S0223-5234(18)30362-3

DOI: [10.1016/j.ejmech.2018.04.028](https://doi.org/10.1016/j.ejmech.2018.04.028)

Reference: EJMECH 10377

To appear in: *European Journal of Medicinal Chemistry*

Received Date: 8 February 2018

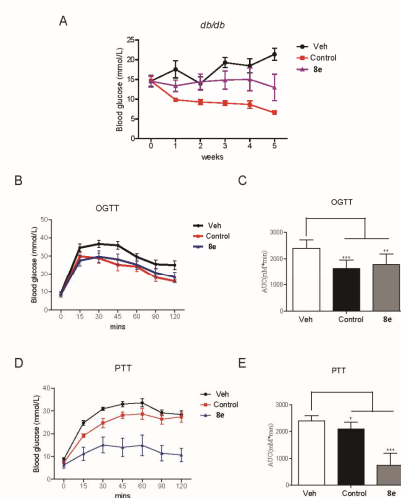
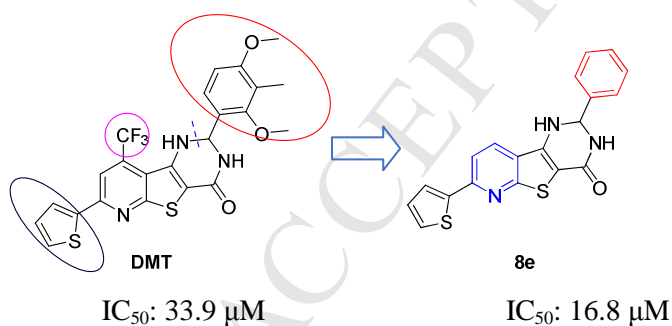
Revised Date: 31 March 2018

Accepted Date: 14 April 2018

Please cite this article as: F. Ma, J. Liu, T. Zhou, M. Lei, J. Chen, X. Wang, Y. Zhang, X. Shen, L. Hu, Discovery and structure-activity relationships study of thieno[2,3-*b*]pyridine analogues as hepatic gluconeogenesis inhibitors, *European Journal of Medicinal Chemistry* (2018), doi: 10.1016/j.ejmech.2018.04.028.

This is a PDF file of an unedited manuscript that has been accepted for publication. As a service to our customers we are providing this early version of the manuscript. The manuscript will undergo copyediting, typesetting, and review of the resulting proof before it is published in its final form. Please note that during the production process errors may be discovered which could affect the content, and all legal disclaimers that apply to the journal pertain.

Graphical Abstract

Discovery and structure-activity relationships study of thieno[2,3-*b*]pyridine analogues as hepatic gluconeogenesis inhibitorsFei Ma^{a,b,c,1}, Jian Liu^{a,1}, Tingting Zhou^{b,d,1}, Min Lei^{b,e}, Jing Chen^{b,e}, Xu Shen^{*}, Lihong Hu^{*}^a Jiangsu Key Laboratory for Functional Substance of Chinese Medicine, Jiangsu Collaborative Innovation Center of Chinese Medicinal Resources Industrialization, State Key Laboratory Cultivation Base for TCM Quality and Efficacy, School of Pharmacy, Nanjing University of Chinese Medicine, Nanjing, 210023, PR China^b State Key Laboratory of Drug Research, Shanghai Institute of Materia Medica, Chinese Academy of Sciences, Shanghai, 201203, China^c Department of Chemistry, Kansas State University, Manhattan, Kansas 66506, United States^d School of Medicine, Jiangnan University, Wuxi 214122, China^e University of Chinese Academy of Sciences, Beijing 100049, China¹ Fei Ma and Jian Liu contributed equally.^{*} Corresponding author: luhu@simm.ac.cn (L. Hu) ; xshen@mail.shcnc.ac.cn (X. Shen)

Discovery and structure-activity relationships study of thieno[2,3-*b*]pyridine analogues as hepatic gluconeogenesis inhibitors

Fei Ma^{a,b,d,1}, Jian Liu^{a,1}, Tingting Zhou^{b,e,1}, Min Lei^{b,c}, Jing Chen^{b,c}, Xiachang Wang^a, Yinan Zhang^a, Xu Shen^{a,*}, Lihong Hu^{a,b,c,*}

^a *Jiangsu Key Laboratory for Functional Substance of Chinese Medicine, Jiangsu Collaborative Innovation Center of Chinese Medicinal Resources Industrialization, State Key Laboratory Cultivation Base for TCM Quality and Efficacy, School of Pharmacy, Nanjing University of Chinese Medicine, Nanjing, 210023, PR China*

^b *State Key Laboratory of Drug Research, Shanghai Institute of Materia Medica, Chinese Academy of Sciences, Shanghai, 201203, China*

^c *University of Chinese Academy of Sciences, Beijing 100049, China*

^d *Department of Chemistry, Kansas State University, Manhattan, Kansas 66506, United States*

^e *School of Medicine, Jiangnan University, Wuxi 214122, China*

¹ Fei Ma, Jian Liu and Tingting Zhou contributed equally.

*Corresponding author: lhhu@simm.ac.cn (L. Hu) ; xshen@simm.ac.cn (X. Shen)

Abstract: Type 2 diabetes mellitus (T2DM) is a chronic, complex and multifactorial metabolic disorder, and targeting gluconeogenesis inhibition is a promising strategy for anti-diabetic drug discovery. This study discovered a new class of thieno[2,3-*b*]pyridine derivatives as hepatic gluconeogenesis inhibitors. First, a hit compound (**DMT**: $IC_{50} = 33.8 \mu\text{M}$) characterized by a thienopyridine core was identified in a cell-based screening of our privileged small molecule library. Structure activity relationships (SARs) study showed that replaced the CF_3 in the thienopyridine core could improve the potency and led to the discovery of **8e** ($IC_{50} = 16.8 \mu\text{M}$) and **9d** ($IC_{50} = 12.3 \mu\text{M}$) with potent inhibition of hepatic glucose production and good drug-like properties. Furthermore, the mechanism of **8e** for the inhibition of hepatic glucose production was also identified, which could be effective through the reductive expression of the mRNA transcription level of gluconeogenic genes, including glucose-6-phosphatase (G6Pase) and hepatic phosphoenolpyruvate carboxykinase (PEPCK). Additionally, **8e** could also reduce the fasting blood glucose and improve the oral glucose tolerance and pyruvate tolerance in *db/db* mice. The optimization of this class of derivatives had provided us a start point to develop new anti-hepatic gluconeogenesis agents.

Keywords: Thieno[2,3-*b*]pyridine derivatives; Structure-activity relationships (SARs); Hepatic gluconeogenesis; Type 2 diabetes mellitus (T2DM).

1. Introduction

Diabetes Mellitus is a serious and increasing global health burden problem [1], and type 2 diabetes mellitus (T2DM) accounts for 90-96% of all cases of diabetes [2]. T2DM is a chronic and multifactorial metabolic disease with complicated pathogenesis characterized by hyperglycemia, insulin resistance and relative lack of insulin [3]. As an important part of glucose metabolism in liver, hepatic gluconeogenesis is responsible for the formation of glucose from non-carbohydrate precursors, such as pyruvate, lactate, lipids, glycerol and glucogenic amino acids [4]. Meanwhile, hepatic gluconeogenesis plays a significant role in maintaining normal plasma glucose levels to avoid hypoglycemia and provide fuels for other organs during prolonged starvation [5]. Hepatic gluconeogenesis is regulated systemically by hormones including insulin and glucagon in response to fasted and fed states [6]. Glucagon could bind to glucagon receptor (GCGR) and activates G α s/cAMP/protein kinase A (PKA)/CREB/CRTC2 signaling pathway to stimulate gluconeogenesis [7,8,9]. On the other hand, insulin could suppress gluconeogenesis through insulin receptor (IR)/IR substrates (IRSs)/phosphatidylinositol-4,5-bisphosphate 3-kinase (PI3K)/protein kinase B (AKT) pathway [10] and salt-inducible kinase 2 (SIK2)/CREB/CRTC2 signaling pathway [11,12]. Two gluconeogenic enzymes, PEPCK and G6Pase, which were highly regulated by glucagon and insulin in correlation with gluconeogenic flux [13,14], have been thought to be rate-limiting enzymes for gluconeogenesis in diabetes [15].

Though a number of anti-diabetic drugs are extensively used in clinic, such as biguanides [16], glucagon-like peptide-1 (GLP-1) analogues [17], dipeptidyl peptidase 4 (DPP4) inhibitors [18,19] and sodium-coupled glucose cotransporter 2 (SGLT2) inhibitors [20,21], many of the available anti-T2DM drugs are facing limited efficacy and long-time tolerability by exhibiting side effects [3]. Therefore, it is urgent to explore novel therapeutic approaches for intervention of T2DM. In patients with T2DM, gluconeogenesis is aberrantly activated, promotes hepatic glucose production and excessively evaluates the blood glucose level [22]. As previous reported, metformin improves hyperglycemia mainly through the suppression of

gluconeogenesis in liver [23]. Hence, regulation of gluconeogenesis and hepatic glucose production could be a promising strategy to regulate blood glucose levels in T2DM [24].

Our research group has been interested in the design, synthesis and biological evaluation of anti-diabetic agents. In a previous cell-based screening of our privileged small molecule library, a thienopyridine derivative (**DMT**, Figure1) with an IC_{50} of 33.8 μ M in the hepatic glucose production assay was discovered. We also found that DMT could inhibit gluconeogenic genes transcription (PEPCK and G6Pase) and efficiently decrease fasting blood glucose and hemoglobin A1c (HbA1c) levels, and improve glucose tolerance and pyruvate tolerance tests in *db/db* mice [25]. Additionally, we identified that DMT antagonized the glucagon-mediated hepatic gluconeogenesis by regulating the $G\alpha_q$ /phospholipase C (PLC)/IP3R-mediated Ca_2^+ /calmodulin (CaM)/PI3K/AKT/forkhead box protein O1 (FOXO1) signaling pathway [25]. All results have highlighted the potency of targeting gluconeogenesis inhibition in the treatment of T2DM and the potential of DMT as an anti-T2DM drug lead compound. To the best of our knowledge, the anti-hepatic glucose production activity of thienopyridine derivatives was first reported. In this manuscript, detailed SAR investigation of DMT was carried out for the purpose of developing compounds with the aim of promoting anti-hepatic glucose production efficacy (Figure 1). As part of ongoing research, herein we report the synthesis, the structure-activity relationship study and preliminary biological evaluation of this new class of anti-hepatic gluconeogenesis agents.

Figure 1

2. Results and discussions

2.1. Chemistry

In this manuscript, the compounds were synthesized (**Scheme 1**). Treatment of ketone **1** with ethyl trifluoroacetate or ethyl acetate under strong basic condition in toluene provided 1,3-diones **2** or **3**, respectively. Condensation of **1** with *N,N*-dimethylformamide dimethyl acetal (DMF-DMA) in DMF afforded enamines

4. Subsequently, the key building blocks pyridine-2-(1*H*)-thiones **6** were prepared by treating 1,3-diones (for R₂=CF₃ and CH₃), enaminones (for R₂=H) and **5** (for R₁=CH₃) with cyanothioacetamide in the presence of triethylamine or triethylenediamine (DABCO). Condensation of **6** with 2-chloro-acetamid yielded the intermediate **7**, which was condensed with corresponding aldehydes through refluxing in AcOH to yield the desired products **8**. In addition, condensation of **6** with corresponding acetamids produced the desired products **9** and **10**, respectively. The compound **11** was synthesized by oxidation of **DMT** with 1,2-dichloro-4,5-dicyanobenzoquinone (DDQ) in THF (**Scheme 2**). Finally, compound **12** was obtained via deamination of **9d** with *tert*-butyl nitrite in DMF (**Scheme 3**). These compounds were assayed for their inhibitory for the anti-hepatic glucose production in long-time fasting primary hepatocytes with the presence of glucagon.

Scheme 1

Scheme 2

Scheme 3

2.2. Biological evaluation

2.2.1. *In vitro* cellular activity and structure-activity relationships

The derivatives were evaluated in the cellular assay measuring the anti-hepatic glucose production potency in long-time fasting primary hepatocytes. Glucagon (10 nM) was used to mimic hyperglucagonemia stimulating excessive gluconeogenesis. **DMT** was used as the positive control. The biological data were listed in **Table 1** and **Table 2**.

Table 1

The inhibition of hepatic glucose production increased significantly (**Table 1**) when induced the electron-drawing group on the benzene ring compared to the lead compound **DMT** (IC₅₀: 24.8 μM for **8a**, 30.2 μM for **8b** and 1.7 μM for **8c**, respectively). Replaced the CF₃ with H atom in the thienopyridine scaffold (IC₅₀: 15.4 μM for **8d** and 16.8 μM for **8e**, respectively), the potency of anti-hepatic glucose production was increased. The result was indicated that electron-drawing group in

thienopyridine scaffold could reduce the potency of anti-hepatic glucose production. When the thiophene group in 2-position of thienopyridine scaffold was replaced by methyl ($IC_{50} > 100 \mu M$ for **8f**), a sharp loss of anti-hepatic glucose production was observed, which implied that an aromatic group was vital in 2-position of thienopyridine scaffold. Given that the chiral center of six-membered ring in **DMT** could bring difficulty on the subsequent drug development, we remove the chiral center of the six-membered ring. First, **DMT** was oxidized by DDQ and obtained compound **11**, which occupied poor water solubility. Therefore, we opened the six-membered ring as the second strategy to remove the chiral center of **DMT**, which led to the discovery of derivatives **9** and **10**.

Table 2

As shown in **Table 2**, the first compound **9a** in this series, containing a amide bond, was found to be equipotent to **8e** in the cell proliferation assay (IC_{50} : $12.3 \mu M$ for **9a** vs $16.8 \mu M$ for **8e**, respectively). This crucial result reinforced the rationale to optimize the series further. The potency of anti-hepatic glucose production decreased with the induction of electro-drawing group in the benzene ring (IC_{50} : $33.4 \mu M$ for **9c** vs $19.1 \mu M$ for **9b**, respectively). Replacing the benzene ring of **9a** with heterocyclic pyridine yielded derivatives **9d** and **9e**, which exhibited equivalently potent inhibition of the hepatic glucose production (IC_{50} : $12.3 \mu M$ for **9d** vs $24.7 \mu M$ for **9e**, respectively). Introducing the halogen group to the aryl ring yielded compound **9f** (IC_{50} : $14.6 \mu M$), which had no significant impact compared to **9a**. In order to investigate the influence of steric hindrance, compound **9g** with 5-aminobenzodioxole was prepared ($IC_{50} > 100 \mu M$ for **9g**), and the result showed that steric hindrance could decreased the potency. Comparison of the cell potency of **9h** and **9i** allowed one to point out that adding hydrophilic group at this position could increase cell penetration and potency as well (IC_{50} : $14.2 \mu M$ for **9i** vs $> 100 \mu M$ for **9h**, respectively). Replacing the benzene ring of **9a** with a hydrophilic aryl ring yielded derivatives **9j** (IC_{50} : $8.04 \mu M$), which exhibited more potent inhibition of the hepatic glucose production compared to **9a**. Based on the structure of **9d**, we synthesized compounds **9k** and **9l** to investigate the effecting of thiophene ring and CF_3 in nucleus core.

Introducing CH₃ to the nucleus core yielded compound **9k** (IC₅₀>100 μM), which showed no potency for the inhibition of hepatic glucose production. The results indicated that increasing the electron in nucleus core could decrease the potency. Furthermore, replacing the thiophene ring with benzene ring yielded **9l** (IC₅₀: 14.4 μM), which could maintain the potency compared to **9d**.

In order to explore the appropriate length between the aryl ring and amide bond, compounds **9m-9o** with one carbon tether were synthesized. The result showed that these derivatives maintained the potency for the inhibition of hepatic glucose production compared to compounds **9a-9c**, respectively. The result described that one carbon tether between the aryl ring and amide bond could maintain the efficiency. Replacing the benzene ring of **9m** with pyrrole ring yielded compound **9p** (IC₅₀: 54.0 μM), which decreased the potency for the inhibition of hepatic glucose production. Additionally, the phenylethylamine-substituted compound **9q** (IC₅₀>100 μM) with two carbon tether between the aryl ring and amide bond showed a significant reduction of potency, which exhibited that two carbon linear chain was negative for the potency.

Table 3

In order to investigate the potency of the *N*-methyl of amide in **9**-series, **10**-series was synthesized and evaluated in hepatic primary cells. **10**-series with *N*-methyl at the amide bond showed the similar SARs compared to the derivatives of **9**-series (Table 3). However, they also exhibited weaker potency for the inhibition of hepatic glucose production.

Among all the potent derivatives with IC₅₀ below 20 μM, the compounds which selected for further biological evaluation and optimization, were not only have potent pharmacological activity, but also with favorable drug-like properties. Therefore, the drug-like properties were taken into account, and we used the ACD-Labs 6.0 to calculate cLog P values. The results demonstrated that the cLog P values of the compounds **8e** and **9d** were lower, these two compounds might have good physicochemical properties. Hence, the compounds **8e** and **9d** were chosen for more extensive in vitro and in vivo anti-diabetic efficacy. However, **9d** was not effective in

the reducing of the key genes G6pase and PEPCK of hepatic gluconeogenesis and was not continued in the following study.

2.2.2. *8e* reduced the mRNA levels of gluconeogenic genes G6Pase, PEPCK in hepatic primary cell

In this assay, the primary hepatocytes were obtained from 9-week-old male C57BL/6 mice. Sodium lactate (20 mM) and sodium pyruvate (2 mM) were used as gluconeogenic substrates, while glucagon (10 nM) was used to stimulate excessive gluconeogenesis mimicking hyperglucagonemia. Incubation of **8e** with glucagon obviously reduced the mRNA levels of gluconeogenic genes G6Pase and PEPCK in dose-dependent manner compared with glucagon treatment results (**Figures 2A** and **2B**), which then inhibited hepatic glucose production in primary hepatocytes.

Figure 2

2.2.3. *In vivo* experiment

Given to the an-hepatic gluconeogenesis potency of **8e** in vitro, we examined its capability in ameliorating hyperglycemia against type 2 diabetic model mice. 8-week-old female mice were divided into 3 groups by fasting blood glucose and body weight. Vehicle or **8e** (25 mg/Kg) was administrated by intraperitoneal injection daily for 5 weeks. Rosiglitazone, a PPAR- γ agonist and clinical effective anti-diabetes drug, used as a positive control, was dosed at 10 mg/kg. Fasting blood glucose levels from 6h fasted mice were measured weekly. The results demonstrated that **8e** treatment could reduce the fasting blood glucose (**Figures. 3A**) in dose-dependent manner. Meanwhile, **8e** could improve the glucose tolerance (**Figures. 3B** and **C**) and pyruvate tolerance (**Figures. 3D** and **E**), respectively. All results indicated that **8e** ameliorated hyperglycemia in *db/db* mice and could be developed as a drug candidate for the treatment of type 2 diabetes patient.

Figure 3

3. Conclusions

In conclusion, novel thieno[2,3-*b*]pyridine analogues were identified as inhibitors of hepatic glucose production. Previous cell-based screening of our privileged small molecule library led to the discovery of **DMT** which characterized by a

thienopyridine core. As we previously reported, DMT antagonized the glucagon-mediated hepatic gluconeogenesis by regulating the Gαq/phospholipase C (PLC)/IP3R-mediated Ca²⁺/calmodulin (CaM)/PI3K/AKT/forkhead box protein O1 (FOXO1) signaling pathway. SARs study on four regions of the **DMT** was carried out to improve its anti-hepatic glucose production potency. The detailed SARs research showed that the eliminating of CF₃ in the nucleus core could improve the potency of anti-hepatic glucose production, and the substituents in benzene ring slightly influenced the activity. The structure modification of **DMT** led to the discovery of two derivatives **8e** and **9d**, which showed good anti-hepatic glucose production potency and excellent drug-like properties. Furthermore, **8e** could also reduce the mRNA levels of gluconeogenic genes in hepatic primary cells, including G6Pase and PEPCK. Additionally, **8e** could also ameliorate hyperglycemia and improve the glucose tolerance and pyruvate tolerance in *db/db* mice. These data indicated that **8e** was a promising drug candidate for the treatment of type 2 diabetes.

4. Experimental section

4.1. Chemistry

4.1.1 General methods

All final compounds are >95% pure based on HPLC. The reagents (chemicals) were purchased from Adamas-beta[®], Alfa Aesar, and Shanghai Chemical Reagent Co. and used without further purification. Nuclear magnetic resonance (NMR) spectroscopy was performed on AMX-400 NMR (IS as TMS). Chemical shifts were reported in parts per million (ppm, δ) downfield from tetramethylsilane. ¹H NMR multiplicity data are denoted by s (singlet), d (doublet), t (triplet), and m (multiplet). HRESIMS were determined on a Micromass Q-Tif Global mass spectrometer and ESI-MS were run on a Bruker Esquire 3000 Plus Spectrometer. Anhydrous solvents were purchased from commercial suppliers.

4.1.2. General procedure for the preparation of compounds **2** and **3**

To a toluene (10 mL) suspension of potassium tert-butoxide (1.35 g, 12 mmol) and methyl ketone (10 mmol) was added dropwise ethyl trifluoroacetate (for **3**) or ethyl acetate (for **4**) at 0 °C. The reaction mixture was allowed to stir for additional 12

h until the starting materials were consumed as determined by LC-MS. Then the solvent was removed under reduced pressure, followed by extracted with ethyl acetate (200 mL) and water (100 mL). The combined organic layers were dried (Na_2SO_4), filtered and the filtrate was concentrated under reduced pressure. The crude product was added to DCM (20 mL) and gave a suspension liquid. The solid precipitate was collected by filtration, washed with DCM and dried under reduced pressure to give the products as yellow solid (63–82%). The precipitate was used without further purification in the next step.

4.1.3. General procedure for the preparation of compounds **4**

To a mixture of aryl ketone **1** (1.1 mL) in anhydrous DMF (20 mL) at room temperature was added *N,N*-dimethylformamide dimethyl acetal (5.0-10.0 equiv). The resulting mixture was warmed to 80 °C and stirred for 2 h. Then the solvent was evaporated under reduced pressure until DMF-DMA was fully removed. The crude products can be straight used for the next step without future purification. Yield: 100%.

4.1.4. General procedure for the preparation of compounds **6**

A mixture of 1,3-diones (**2**, **3** or **5**) (1 mmol) in anhydrous ethanol (2 mL) at room temperature was added Et_3N (30 μL) and cyanothioacetamide (120 mg, 1.2 mmol). The resulting mixture was warmed to 80 °C and stirred for 2 h. Then the solvent was evaporated under reduced pressure. The crude products **6** can be straight used for the next step without future purification.

To a mixture of compound **4** (1 mmol) in anhydrous ethanol (2 mL) at room temperature was added DABCO (168 mg, 1.5 mmol) and cyanothioacetamide (120 mg, 1.2 mmol). The resulting mixture was warmed to 80 °C and stirred for 2 h. Then the solvent was evaporated under reduced pressure. The crude products **6** can be straight used for the next step without future purification.

4.1.5. General procedure for the preparation of *DMT* and compounds **8**

To a solution of crude products **6** from above procedure in DMF (3 mL) added aqueous 10% KOH solution (3 mL) followed by the addition of 2-chloro-acetamid at room temperature. The resulting mixture was stirred overnight at room temperature.

Then H₂O (3 mL) was added to the mixture so that the desired product can be precipitated. The solid precipitate was collected by filtration, washed with MeOH (2 mL) and dried under reduced pressure to give the products **7** as yellow solid in 90% yield. To a mixture of compound **7** (0.5 mmol) in AcOH (2 mL) at room temperature added corresponding aldehydes (0.75 mmol). The resulting mixture was stirred and warmed to 100 °C to reflux. Once the reaction was completed as indicated by LC-MS, the reaction mixture was concentrated under vacuum and MeOH (2 mL) was added to give a suspension liquid. The solid precipitate was collected by filtration, washed with MeOH (2 mL) and dried under reduced pressure to give the desired products **DMT** and **8a-8f** as yellow solid.

4.1.5.1

2-(2,4-dimethoxy-3-methylphenyl)-7-(thiophen-2-yl)-9-(trifluoromethyl)-2,3-dihydropyrido[3',2':4,5]thieno[3,2-d]pyrimidin-4(1H)-one (DMT)

Yellow solid; Yield 85%; ¹H NMR (400 MHz, DMSO-*d*₆) δ 8.39 (d, *J* = 2.6 Hz, 1H), 8.31 (s, 1H), 8.23–8.20 (m, 1H), 7.86–7.83 (m, 1H), 7.25 (dd, *J* = 8.6, 3.6 Hz, 2H), 6.76 (d, *J* = 8.7 Hz, 1H), 6.15 (dd, *J* = 6.0, 2.7 Hz, 1H), 5.95 (d, *J* = 6.1 Hz, 1H), 3.77 (s, 3H), 3.76 (s, 3H), 2.08 (s, 3H); ¹³C NMR (151 MHz, DMSO-*d*₆) δ 162.49, 161.10, 158.54, 156.43, 151.84, 142.12, 141.37, 132.27 and 132.05 and 131.82 and 131.60 (q, ²*J*_{CF} = 33.9 Hz), 131.22, 129.09, 129.04, 124.92 (2C), 125.15 and 123.33 and 121.51 and 119.70 (q, ¹*J*_{CF} = 274.2 Hz), 118.91, 118.12, 112.79 and 112.76 and 112.72 and 112.67 (q, ³*J*_{CF} = 5.2 Hz), 112.31, 105.98, 62.74, 61.21, 55.58, 9.07; ESI-MS *m/z*: 506.4 [M+H]⁺; HRMS (ESI) *m/z* calcd for C₂₃H₁₉F₃N₃O₂S₂⁺ [M+H]⁺: 506.0814; found: 506.0807.

4.1.5.2

2-phenyl-7-(thiophen-2-yl)-9-(trifluoromethyl)-2,3-dihydropyrido[3',2':4,5]thieno[3,2-d]pyrimidin-4(1H)-one (8a). Yellow solid; Yield 64%; ¹H NMR (400 MHz, DMSO-*d*₆) δ 8.83 (d, *J* = 4.1 Hz, 1H), 8.32 (s, 1H), 8.20 (dd, *J* = 3.8, 1.0 Hz, 1H), 7.84 (dd, *J* = 5.0, 1.0 Hz, 1H), 7.49 (d, *J* = 7.6 Hz, 2H), 7.35–7.31 (m, 2H), 7.29–7.23 (m, 2H), 6.68 (d, *J* = 6.2 Hz, 1H), 6.01–5.95 (dd, *J* = 6.2, 4.1 Hz, 1H); ¹³C NMR (126 MHz, DMSO-*d*₆) δ 162.47, 160.49, 151.91, 142.14, 141.93, 140.70, 132.51 and

132.25 and 131.98 and 131.71 (q, $^2J_{CF} = 33.6$ Hz), 131.22, 129.08, 129.03, 128.17 (2C), 127.88, 125.87 (2C), 125.79 and 123.61 and 121.43 and 119.25 (q, $^1J_{CF} = 274.7$ Hz), 118.18, 112.72 and 112.68 and 112.63 and 112.59 (q, $^3J_{CF} = 5.6$ Hz), 112.13, 64.91; ESI-MS m/z : 432.6 $[M+H]^+$; HRMS (ESI) m/z calcd for $C_{20}H_{13}F_3N_3OS_2^+$ $[M+H]^+$: 432.0447; found: 432.0441.

4.1.5.3

2-(4-hydroxy-3-methoxyphenyl)-7-(thiophen-2-yl)-9-(trifluoromethyl)-2,3-dihydropyrido[3',2':4,5]thieno[3,2-d]pyrimidin-4(1H)-one (**8b**). Yellow solid; Yield 87%; 1H NMR (400 MHz, DMSO- d_6) δ 8.98 (s, 1H), 8.72 (d, $J = 3.8$ Hz, 1H), 8.31 (s, 1H), 8.21 (dd, $J = 3.8, 0.9$ Hz, 1H), 7.83 (dd, $J = 5.0, 0.9$ Hz, 1H), 7.25 (dd, $J = 5.0, 3.8$ Hz, 1H), 7.10 (d, $J = 1.9$ Hz, 1H), 6.86 (dd, $J = 8.2, 1.9$ Hz, 1H), 6.70 (d, $J = 8.2$ Hz, 1H), 6.50 (d, $J = 6.2$ Hz, 1H), 5.87 (dd, $J = 6.2, 3.8$ Hz, 1H), 3.69 (s, 3H); ^{13}C NMR (126 MHz, DMSO- d_6) δ 162.42, 160.62, 151.80, 147.34, 146.36, 142.16, 140.71, 132.43 and 132.17 and 131.90 and 131.63 (q, $^2J_{CF} = 33.4$ Hz), 132.40, 131.16, 129.04, 129.02, 125.82 and 123.64 and 121.46 and 119.28 (q, $^1J_{CF} = 274.6$ Hz), 118.48, 118.30, 114.73, 112.70 and 112.65 and 112.61 and 112.56 (q, $^3J_{CF} = 6.1$ Hz), 112.42, 110.12, 65.06, 55.31; ESI-MS m/z : 478.7 $[M+H]^+$; HRMS (ESI) m/z calcd for $C_{21}H_{15}F_3N_3O_3S_2^+$ $[M+H]^+$: 478.0501; found: 478.0512.

4.1.5.4

2-(4-nitrophenyl)-7-(thiophen-2-yl)-9-(trifluoromethyl)-2,3-dihydropyrido[3',2':4,5]thieno[3,2-d]pyrimidin-4(1H)-one (**8c**). Yellow solid; Yield 85%; 1H NMR (400 MHz, DMSO- d_6) δ 8.99 (d, $J = 4.4$ Hz, 1H), 8.33 (s, 1H), 8.24–8.18 (m, 3H), 7.84 (dd, $J = 4.9, 1.0$ Hz, 1H), 7.73 (d, $J = 8.7$ Hz, 2H), 7.25 (dd, $J = 4.9, 3.9$ Hz, 1H), 6.89 (d, $J = 6.6$ Hz, 1H), 6.10 (dd, $J = 6.6, 4.4$ Hz, 1H); ^{13}C NMR (126 MHz, DMSO- d_6) δ 162.52, 160.10, 152.11, 149.72, 147.26, 142.09, 140.51, 132.62 and 132.35 and 132.08 and 131.81 (q, $^2J_{CF} = 34.0$ Hz), 131.35, 129.23, 129.07, 127.22 (2C), 125.77 and 123.59 and 121.41 and 119.28 (q, $^1J_{CF} = 271.5$ Hz), 123.47 (2C), 118.14, 112.84 and 112.80 and 112.76 and 112.72 (q, $^3J_{CF} = 4.9$ Hz), 112.49, 64.40; ESI-MS m/z : 477.7 $[M+H]^+$; HRMS (ESI) m/z calcd for $C_{20}H_{12}F_3N_4O_3S_2^+$ $[M+H]^+$: 477.0297; found: 477.0287.

4.1.5.5

2-(2,4-dimethoxy-3-methylphenyl)-7-(thiophen-2-yl)-2,3-dihydropyrido[3',2':4,5]thieno[3,2-d]pyrimidin-4(1H)-one (**8d**). Yellow solid; Yield 72%; ^1H NMR (400 MHz, DMSO- d_6) δ 8.41 (d, $J = 8.6$ Hz, 1H), 8.00 (d, $J = 8.6$ Hz, 1H), 7.94 (dd, $J = 3.7, 1.0$ Hz, 1H), 7.89 (s, 1H), 7.84 (s, 1H), 7.74 (dd, $J = 5.0, 1.0$ Hz, 1H), 7.55 (d, $J = 8.7$ Hz, 1H), 7.21 (dd, $J = 5.0, 3.7$ Hz, 1H), 6.89 (d, $J = 8.7$ Hz, 1H), 6.16 (s, 1H), 3.81 (s, 3H), 3.74 (s, 3H), 2.11 (s, 3H); ^{13}C NMR (126 MHz, DMSO- d_6) δ 162.48, 161.31, 158.79, 156.83, 152.02, 145.55, 143.64, 132.12, 129.74, 128.73, 127.07, 126.42, 124.14, 122.80, 118.39, 115.31, 106.63, 103.01, 63.11, 61.67, 55.75, 9.07; ESI-MS m/z : 438.6 $[\text{M}+\text{H}]^+$; HRMS (ESI) m/z calcd for $\text{C}_{22}\text{H}_{20}\text{N}_3\text{O}_3\text{S}_2^+$ $[\text{M}+\text{H}]^+$: 438.0941; found: 438.0945.

4.1.5.6

2-phenyl-7-(thiophen-2-yl)-2,3-dihydropyrido[3',2':4,5]thieno[3,2-d]pyrimidin-4(1H)-one (**8e**). Yellow solid; Yield 61%; ^1H NMR (400 MHz, DMSO- d_6) δ 8.44 (d, $J = 8.6$ Hz, 1H), 8.21 (d, $J = 10.7$ Hz, 2H), 8.03 (d, $J = 8.6$ Hz, 1H), 7.95 (d, $J = 3.2$ Hz, 1H), 7.75 (d, $J = 5.0$ Hz, 1H), 7.60 (d, $J = 10.7$ Hz, 2H), 7.48–7.37 (m, 3H), 7.25–7.19 (m, 1H), 5.99 (s, 1H); ^{13}C NMR (126 MHz, DMSO- d_6) δ 161.98, 161.27, 152.07, 145.05, 143.61, 140.17, 132.01, 129.77, 128.80, 128.73, 128.39 (2C), 127.20 (2C), 127.09, 122.79, 115.37, 103.03, 68.07; ESI-MS m/z : 364.6 $[\text{M}+\text{H}]^+$; HRMS (ESI) m/z calcd for $\text{C}_{19}\text{H}_{14}\text{N}_3\text{O}_2\text{S}^+$ $[\text{M}+\text{H}]^+$: 364.0573; found: 364.0579.

4.1.5.7

2-(2,4-dimethoxy-3-methylphenyl)-7-methyl-9-(trifluoromethyl)-2,3-dihydropyrido[3',2':4,5]thieno[3,2-d]pyrimidin-4(1H)-one (**8f**). Yellow solid; Yield 68%; ^1H NMR (400 MHz, DMSO- d_6) δ 8.34 (d, $J = 2.6$ Hz, 1H), 7.76 (s, 1H), 7.23 (d, $J = 8.7$ Hz, 1H), 6.74 (d, $J = 8.7$ Hz, 1H), 6.13 (dd, $J = 5.8, 2.6$ Hz, 1H), 5.91 (d, $J = 5.8$ Hz, 1H), 3.76 (s, 3H), 3.75 (s, 3H), 2.69 (s, 3H), 2.07 (s, 3H); ^{13}C NMR (126 MHz, DMSO- d_6) δ 162.22, 161.21, 159.58, 158.51, 156.42, 141.24, 131.44 and 131.17 and 130.91 and 130.64 (q, $^2J_{\text{CF}} = 33.7$ Hz), 125.80 and 123.62 and 121.44 and 119.27 (q, $^1J_{\text{CF}} = 274.1$ Hz), 124.93, 124.89, 118.89, 117.60, 117.16 and 117.12 and 117.08 and 117.03 (q, $^3J_{\text{CF}} = 5.6$ Hz), 111.78, 105.96, 62.75, 61.19, 55.57, 24.08, 9.05; ESI-MS m/z : 438.6

[M+H]⁺; HRMS (ESI) m/z calcd for C₂₀H₁₉F₃N₃O₃S⁺ [M+H]⁺: 438.1094; found: 438.1085.

4.1.6. General procedure for the preparation of compounds **9** and **10**

To a solution of crude products **6** from above procedure in DMF (3 mL) added aqueous 10% KOH solution (3 mL) followed by the addition of chloroacetamides (for **9** and **10**, respectively) at room temperature. The resulting mixture was stirred overnight at room temperature. Then H₂O (3 mL) was added to the mixture so that the desired product can be precipitated. The solid precipitate was collected by filtration, washed with MeOH (2 mL) and dried under reduced pressure to obtain the products **9** and **10** as yellow solid.

4.1.6.1 3-amino-*N*-phenyl-6-(thiophen-2-yl)thieno[2,3-*b*]pyridine-2-carboxamide (**9a**).

Yellow solid; Yield 47% (two steps); ¹H NMR (400 MHz, DMSO-*d*₆) δ 9.45 (s, 1H), 8.52 (d, *J* = 8.6 Hz, 1H), 8.04 (d, *J* = 8.6 Hz, 1H), 7.97 (d, *J* = 3.6 Hz, 1H), 7.75 (d, *J* = 5.0 Hz, 1H), 7.69 (d, *J* = 7.8 Hz, 2H), 7.40 (s, 2H), 7.33 (t, *J* = 7.8 Hz, 2H), 7.23 (dd, *J* = 5.0, 3.6 Hz, 1H), 7.08 (t, *J* = 7.3 Hz, 1H); ¹³C NMR (126 MHz, DMSO-*d*₆) δ 163.80, 158.64, 152.54, 146.92, 143.67, 138.92, 131.68, 129.60, 128.71, 128.41 (2C), 126.99, 124.62, 123.45, 121.23 (2C), 115.14, 96.50; ESI-MS m/z : 352.6 [M+H]⁺; HRMS (ESI) m/z calcd for C₁₈H₁₄N₃OS₂⁺ [M+H]⁺: 352.0573; found: 352.0565.

4.1.6.2

3-amino-*N*-(4-methoxyphenyl)-6-(thiophen-2-yl)thieno[2,3-*b*]pyridine-2-carboxamide (**9b**). Yellow solid; Yield 49% (two steps); ¹H NMR (400 MHz, DMSO-*d*₆) δ 9.35 (s, 1H), 8.50 (d, *J* = 8.6 Hz, 1H), 8.03 (d, *J* = 8.6 Hz, 1H), 7.96 (d, *J* = 3.4 Hz, 1H), 7.74 (d, *J* = 4.9 Hz, 1H), 7.57 (d, *J* = 9.0 Hz, 2H), 7.35 (s, 2H), 7.23 (dd, *J* = 4.9, 3.4 Hz, 1H), 6.91 (d, *J* = 9.0 Hz, 2H), 3.74 (s, 3H); ¹³C NMR (126 MHz, DMSO-*d*₆) δ 163.60, 158.57, 155.56, 152.40, 146.53, 143.70, 131.79, 131.59, 129.53, 128.70, 126.92, 124.69, 123.07 (2C), 115.10, 113.57 (2C), 96.70, 55.16; ESI-MS m/z : 382.6 [M+H]⁺; HRMS (ESI) m/z calcd for C₁₉H₁₆N₃O₂S₂⁺ [M+H]⁺: 382.0678; found: 382.0673.

4.1.6.3

3-amino-*N*-(4-nitrophenyl)-6-(thiophen-2-yl)thieno[2,3-*b*]pyridine-2-carboxamide (**9c**). Yellow solid; Yield 49% (two steps); ¹H NMR (400 MHz, DMSO-*d*₆) δ 10.03 (s,

1H), 8.57 (d, $J = 8.6$ Hz, 1H), 8.24 (d, $J = 9.3$ Hz, 2H), 8.06 (d, $J = 8.6$ Hz, 1H), 8.03 (d, $J = 9.3$ Hz, 2H), 7.99 (dd, $J = 3.8, 1.0$ Hz, 1H), 7.76 (dd, $J = 5.0, 1.0$ Hz, 1H), 7.62 (s, 2H), 7.23 (dd, $J = 5.0, 3.8$ Hz, 1H); ^{13}C NMR (126 MHz, DMSO- d_6) δ 164.08, 158.96, 153.04, 148.39, 145.74, 143.53, 142.00, 131.99, 129.84, 128.75, 127.25, 124.59 (2C), 124.26, 120.05 (2C), 115.29, 95.48; ESI-MS m/z : 397.6 $[\text{M}+\text{H}]^+$; HRMS (ESI) m/z calcd for $\text{C}_{18}\text{H}_{13}\text{N}_4\text{O}_3\text{S}_2^+$ $[\text{M}+\text{H}]^+$: 397.0424; found: 397.0412.

4.1.6.4

3-amino-N-(pyridin-4-yl)-6-(thiophen-2-yl)thieno[2,3-b]pyridine-2-carboxamide (9d). Yellow solid; Yield 61% (two steps); ^1H NMR (400 MHz, DMSO- d_6) δ 9.78 (s, 1H), 8.56 (d, $J = 8.6$ Hz, 1H), 8.43 (d, $J = 6.1$ Hz, 2H), 8.05 (d, $J = 8.6$ Hz, 1H), 7.98 (d, $J = 3.8$ Hz, 1H), 7.79–7.73 (m, 3H), 7.58 (s, 2H), 7.23 (dd, $J = 5.0, 3.8$ Hz, 1H); ^{13}C NMR (126 MHz, DMSO- d_6) δ 164.32, 158.90, 152.99, 149.97 (2C), 148.19, 146.14, 143.54, 131.97, 129.80, 128.75, 127.22, 124.30, 115.28, 114.30 (2C), 95.50; ESI-MS m/z : 353.6 $[\text{M}+\text{H}]^+$; HRMS (ESI) m/z calcd for $\text{C}_{17}\text{H}_{13}\text{N}_4\text{OS}_2^+$ $[\text{M}+\text{H}]^+$: 353.0525; found: 353.0529.

4.1.6.5

3-amino-N-(pyridin-2-yl)-6-(thiophen-2-yl)thieno[2,3-b]pyridine-2-carboxamide (9e). Yellow solid; Yield 53% (two steps); ^1H NMR (400 MHz, DMSO- d_6) δ 9.71 (s, 1H), 8.54 (d, $J = 8.6$ Hz, 1H), 8.36 (d, $J = 3.7$ Hz, 1H), 8.07 (d, $J = 8.3$ Hz, 1H), 8.04 (d, $J = 8.6$ Hz, 1H), 7.97 (d, $J = 3.1$ Hz, 1H), 7.86–7.77 (m, 1H), 7.75 (d, $J = 4.9$ Hz, 1H), 7.48 (s, 2H), 7.23 (dd, $J = 4.9, 3.7$ Hz, 1H), 7.17–7.09 (m, 1H); ^{13}C NMR (126 MHz, DMSO- d_6) δ 163.90, 158.89, 152.76, 152.01, 147.88, 147.58, 143.67, 137.92, 131.91, 129.75, 128.75, 127.11, 124.51, 119.42, 115.12, 114.81, 96.47; ESI-MS m/z : 353.6 $[\text{M}+\text{H}]^+$; HRMS (ESI) m/z calcd for $\text{C}_{17}\text{H}_{13}\text{N}_4\text{OS}_2^+$ $[\text{M}+\text{H}]^+$: 353.0525; found: 353.0528.

4.1.6.6

3-amino-N-(4-chloro-3-(trifluoromethyl)phenyl)-6-(thiophen-2-yl)thieno[2,3-b]pyridine-2-carboxamide (9f). Yellow solid; Yield 63% (two steps); ^1H NMR (400 MHz, DMSO- d_6) δ 9.83 (s, 1H), 8.55 (d, $J = 8.6$ Hz, 1H), 8.35 (d, $J = 2.4$ Hz, 1H), 8.08–8.00 (m, 2H), 7.99–7.93 (m, 1H), 7.77–7.72 (m, 1H), 7.67 (d, $J = 8.8$ Hz, 1H), 7.54 (s,

2H), 7.22 (dd, $J = 5.0, 3.8$ Hz, 1H); ^{13}C NMR (126 MHz, DMSO- d_6) δ 164.00, 158.83, 152.88, 147.95, 143.56, 138.71, 131.90, 131.71, 129.73, 128.72, 127.15, 126.78 and 126.54 and 126.30 and 126.05 (q, $^2J_{CF} = 30.5$ Hz), 126.11 and 124.37 and 121.77 and 119.60 (q, $^1J_{CF} = 245.9$ Hz), 125.35, 123.94, 123.79, 119.44 and 119.40 and 119.36 and 119.31 (q, $^3J_{CF} = 5.2$ Hz), 115.25, 95.36; ESI-MS m/z : 454.6 $[\text{M}+\text{H}]^+$; HRMS (ESI) m/z calcd for $\text{C}_{19}\text{H}_{12}\text{ClF}_3\text{N}_3\text{OS}_2^+ [\text{M}+\text{H}]^+$: 454.0057; found: 454.0045.

4.1.6.7

3-amino-N-(benzo[d][1,3]dioxol-5-yl)-6-(thiophen-2-yl)thieno[2,3-b]pyridine-2-carboxamide (9g). Yellow solid; Yield 59% (two steps); ^1H NMR (400 MHz, DMSO- d_6) δ 9.35 (s, 1H), 8.50 (d, $J = 8.6$ Hz, 1H), 8.02 (d, $J = 8.6$ Hz, 1H), 7.97–7.93 (m, 1H), 7.76–7.71 (m, 1H), 7.35 (s, 2H), 7.34 (d, $J = 2.0$ Hz, 1H), 7.22 (dd, $J = 4.9, 3.8$ Hz, 1H), 7.10 (dd, $J = 8.4, 2.0$ Hz, 1H), 6.88 (d, $J = 8.4$ Hz, 1H), 6.01 (s, 2H); ^{13}C NMR (126 MHz, DMSO- d_6) δ 163.64, 158.58, 152.46, 146.84, 146.71, 143.67, 143.21, 133.06, 131.62, 129.56, 128.70, 126.95, 124.63, 115.12, 114.37, 107.73, 103.52, 100.95, 96.47; ESI-MS m/z : 396.6 $[\text{M}+\text{H}]^+$; HRMS (ESI) m/z calcd for $\text{C}_{19}\text{H}_{14}\text{N}_3\text{O}_3\text{S}_2^+ [\text{M}+\text{H}]^+$: 396.0471; found: 396.0464.

4.1.6.8 3-amino-N-cyclohexyl-6-(thiophen-2-yl)thieno[2,3-b]pyridine-2-carboxamide (9h). Yellow solid; Yield 45% (two steps); ^1H NMR (400 MHz, DMSO- d_6) δ 8.43 (d, $J = 8.5$ Hz, 1H), 7.99 (d, $J = 8.5$ Hz, 1H), 7.93 (d, $J = 3.6$ Hz, 1H), 7.72 (d, $J = 5.0$ Hz, 1H), 7.41 (d, $J = 8.1$ Hz, 1H), 7.21 (dd, $J = 5.0, 3.6$ Hz, 1H), 7.16 (s, 2H), 3.81–3.68 (m, 1H), 1.84–1.68 (m, 4H), 1.65–1.55 (m, 1H), 1.32 (tt, $J = 20.5, 10.5$ Hz, 4H), 1.17–1.05 (m, 1H); ^{13}C NMR (126 MHz, DMSO- d_6) δ 164.05, 158.26, 152.00, 145.25, 143.75, 131.35, 129.31, 128.64, 126.71, 124.91, 114.95, 97.52, 48.13, 32.45 (2C), 25.25, 25.16 (2C); ESI-MS m/z : 358.6 $[\text{M}+\text{H}]^+$; HRMS (ESI) m/z calcd for $\text{C}_{18}\text{H}_{20}\text{N}_3\text{OS}_2^+ [\text{M}+\text{H}]^+$: 358.1042; found: 358.1048.

4.1.6.9

3-amino-N-(piperidin-4-yl)-6-(thiophen-2-yl)thieno[2,3-b]pyridine-2-carboxamide hydrochloride (9i). Yellow solid; Yield 53% (two steps); ^1H NMR (400 MHz, DMSO- d_6) δ 9.04 (d, $J = 11.9$ Hz, 1H), 8.93 (d, $J = 11.9$ Hz, 1H), 8.48 (d, $J = 8.5$ Hz, 1H), 7.99 (d, $J = 8.5$ Hz, 1H), 7.96–7.89 (m, 1H), 7.78 (d, $J = 7.2$ Hz, 1H), 7.72 (d, J

= 4.7 Hz, 1H), 7.26–7.16 (m, 1H), 5.22–3.58 (m, 3H), 3.30 (d, $J = 10.9$ Hz, 2H), 2.96 (q, $J = 10.9$ Hz, 2H), 2.00–1.76 (m, 4H); ^{13}C NMR (126 MHz, DMSO- d_6) δ 164.57, 158.43, 152.21, 145.79, 143.70, 131.54, 129.43, 128.69, 126.85, 124.75, 115.02, 96.89, 44.38, 42.38 (2C), 28.30 (2C); ESI-MS m/z : 359.6 $[\text{M-HCl}+\text{H}]^+$; HRMS (ESI) m/z calcd for $\text{C}_{17}\text{H}_{19}\text{N}_4\text{OS}_2^+$ $[\text{M-HCl}+\text{H}]^+$: 359.0995; found: 359.0986.

4.1.6.10

3-amino-N-(4-(2-(4-methylpiperazin-1-yl)ethoxy)phenyl)-6-(thiophen-2-yl)thieno[2,3-b]pyridine-2-carboxamide (9j). Yellow solid; Yield 59% (two steps); ^1H NMR (400 MHz, DMSO- d_6) δ 9.37 (s, 1H), 8.54 (d, $J = 8.5$ Hz, 1H), 8.03 (d, $J = 8.5$ Hz, 1H), 7.96 (d, $J = 3.2$ Hz, 1H), 7.74 (d, $J = 4.9$ Hz, 1H), 7.58 (d, $J = 8.8$ Hz, 2H), 7.36 (s, 2H), 7.28–7.18 (m, 1H), 6.93 (d, $J = 8.8$ Hz, 2H), 3.12–2.58 (m, 15H); ^{13}C NMR (126 MHz, DMSO- d_6) δ 163.61, 158.56, 154.59, 152.41, 146.58, 143.68, 131.65, 129.61, 129.56, 128.72, 126.96, 124.68, 123.01 (2C), 115.11, 114.26 (2C), 96.63, 65.54, 55.66, 52.43 (2C), 49.62 (2C), 45.39; ESI-MS m/z : 494.6 $[\text{M}+\text{H}]^+$; HRMS (ESI) m/z calcd for $\text{C}_{25}\text{H}_{28}\text{N}_5\text{O}_2\text{S}_2^+$ $[\text{M}+\text{H}]^+$: 494.1679; found: 494.1675.

4.1.6.11

3-amino-4-methyl-N-(pyridin-4-yl)-6-(thiophen-2-yl)thieno[2,3-b]pyridine-2-carboxamide (9k). Yellow solid; Yield 53% (two steps); ^1H NMR (400 MHz, DMSO- d_6) δ 9.80 (s, 1H), 8.43 (d, $J = 5.9$ Hz, 2H), 7.94 (d, $J = 3.5$ Hz, 1H), 7.79 (s, 1H), 7.74 (m, 3H), 7.23 (dd, $J = 5.0, 3.5$ Hz, 1H), 7.15 (s, 2H), 2.84 (s, 3H); ^{13}C NMR (126 MHz, DMSO- d_6) δ 164.66, 159.50, 152.34, 150.19, 150.03 (2C), 146.05, 145.89, 143.28, 129.68, 128.69, 127.04, 123.42, 117.32, 114.46 (2C), 96.62, 20.15; ESI-MS m/z : 367.6 $[\text{M}+\text{H}]^+$; HRMS (ESI) m/z calcd for $\text{C}_{18}\text{H}_{15}\text{N}_4\text{OS}_2^+$ $[\text{M}+\text{H}]^+$: 367.0682; found: 367.0686.

4.1.6.12 *3-amino-6-phenyl-N-(pyridin-4-yl)thieno[2,3-b]pyridine-2-carboxamide (9l)*

Yellow solid; Yield 34% (three steps); ^1H NMR (400 MHz, DMSO- d_6) δ 9.81 (s, 1H), 8.63 (d, $J = 8.6$ Hz, 1H), 8.44 (dd, $J = 4.9, 1.4$ Hz, 2H), 8.23–8.17 (m, 2H), 8.10 (d, $J = 8.6$ Hz, 1H), 7.78 (dd, $J = 4.9, 1.4$ Hz, 2H), 7.61 (s, 2H), 7.58–7.48 (m, 3H); ^{13}C NMR (126 MHz, DMSO- d_6) δ 164.40, 159.25, 157.25, 150.00 (2C), 148.10, 146.13, 137.77, 132.16, 129.82, 128.91 (2C), 127.07 (2C), 124.64, 116.54, 114.27 (2C),

95.78; ESI-MS m/z : 347.6 $[M+H]^+$; HRMS (ESI) m/z calcd for $C_{19}H_{15}N_4OS^+$ $[M+H]^+$: 347.0961; found: 347.0956.

4.1.6.13 *3-amino-N-benzyl-6-(thiophen-2-yl)thieno[2,3-b]pyridine-2-carboxamide* (**9m**). Yellow solid; Yield 71% (two steps); 1H NMR (400 MHz, DMSO- d_6) δ 8.46 (d, $J = 8.6$ Hz, 1H), 8.30 (t, $J = 6.0$ Hz, 1H), 8.01 (d, $J = 8.6$ Hz, 1H), 7.94 (dd, $J = 5.0, 3.6$ Hz, 1H), 7.73 (dd, $J = 5.0, 3.6$ Hz, 1H), 7.34–7.31 (m, 4H), 7.25–7.20 (m, 4H), 4.43 (d, $J = 6.0$ Hz, 2H); ^{13}C NMR (126 MHz, DMSO- d_6) δ 164.87, 158.29, 152.16, 145.60, 143.73, 140.07, 131.49, 129.41, 128.66, 128.20 (2C), 127.21 (2C), 126.79, 126.62, 124.88, 115.02, 96.88, 42.30; ESI-MS m/z : 366.6 $[M+H]^+$; HRMS (ESI) m/z calcd for $C_{19}H_{16}N_3OS_2^+$ $[M+H]^+$: 366.0729; found: 366.0724.

4.1.6.14

3-amino-N-(4-methoxybenzyl)-6-(thiophen-2-yl)thieno[2,3-b]pyridine-2-carboxamide (**9n**). Yellow solid; Yield 57% (two steps); 1H NMR (400 MHz, DMSO- d_6) δ 8.45 (d, $J = 8.5$ Hz, 1H), 8.24 (t, $J = 6.0$ Hz, 1H), 8.00 (d, $J = 8.5$ Hz, 1H), 7.93 (d, $J = 3.6$ Hz, 1H), 7.72 (d, $J = 5.0$ Hz, 1H), 7.25 (d, $J = 8.6$ Hz, 2H), 7.21 (m, 3H), 6.89 (d, $J = 8.6$ Hz, 2H), 4.35 (d, $J = 6.0$ Hz, 2H), 3.72 (s, 3H); ^{13}C NMR (126 MHz, DMSO- d_6) δ 164.75, 158.27, 158.11, 152.12, 145.51, 143.73, 132.04, 131.47, 129.39, 128.66, 128.61 (2C), 126.78, 124.89, 115.01, 113.61 (2C), 97.00, 55.04, 41.73; ESI-MS m/z : 396.6 $[M+H]^+$; HRMS (ESI) m/z calcd for $C_{20}H_{18}N_3O_2S_2^+$ $[M+H]^+$: 396.0835; found: 396.0841.

4.1.6.15

3-amino-N-(4-nitrobenzyl)-6-(thiophen-2-yl)thieno[2,3-b]pyridine-2-carboxamide (**9o**). Yellow solid; Yield 62% (two steps); 1H NMR (400 MHz, DMSO- d_6) δ 8.46 (m, 2H), 8.22 (d, $J = 8.7$ Hz, 2H), 8.02 (d, $J = 8.6$ Hz, 1H), 7.95 (d, $J = 2.9$ Hz, 1H), 7.73 (d, $J = 5.0$ Hz, 1H), 7.58 (d, $J = 8.7$ Hz, 2H), 7.25 (s, 2H), 7.21 (dd, $J = 5.0, 2.9$ Hz, 1H), 4.54 (d, $J = 5.8$ Hz, 2H); ^{13}C NMR (126 MHz, DMSO- d_6) δ 165.05, 158.33, 152.31, 148.20, 146.36, 145.94, 143.68, 131.59, 129.48, 128.68, 128.18 (2C), 126.87, 124.79, 123.48 (2C), 115.08, 96.36, 42.10; ESI-MS m/z : 411.6 $[M+H]^+$; HRMS (ESI) m/z calcd for $C_{19}H_{15}N_4O_3S_2^+$ $[M+H]^+$: 411.0580; found: 411.0585.

4.1.6.16

3-amino-N-(furan-2-ylmethyl)-6-(thiophen-2-yl)thieno[2,3-b]pyridine-2-carboxamide (9p). Yellow solid; Yield 68% (two steps); ^1H NMR (400 MHz, $\text{DMSO-}d_6$) δ 8.46 (d, $J = 8.6$ Hz, 1H), 8.22 (t, $J = 5.7$ Hz, 1H), 8.00 (d, $J = 8.6$ Hz, 1H), 7.94 (dd, $J = 3.6$, 1.0 Hz, 1H), 7.73 (dd, $J = 5.0$, 1.0 Hz, 1H), 7.58 (d, $J = 1.9$ Hz, 1H), 7.28–7.17 (m, 3H), 6.40 (dd, $J = 3.0$, 1.9 Hz, 1H), 6.25 (d, $J = 3.0$ Hz, 1H), 4.41 (d, $J = 5.7$ Hz, 2H); ^{13}C NMR (126 MHz, $\text{DMSO-}d_6$) δ 164.75, 158.37, 152.83, 152.22, 145.77, 143.73, 141.83, 131.54, 129.45, 128.68, 126.83, 124.80, 115.03, 110.47, 106.76, 96.71, 35.67; ESI-MS m/z : 356.6 $[\text{M}+\text{H}]^+$; HRMS (ESI) m/z calcd for $\text{C}_{17}\text{H}_{14}\text{N}_3\text{O}_2\text{S}_2^+$ $[\text{M}+\text{H}]^+$: 356.0522; found: 356.0527.

4.1.6.17 3-amino-N-phenethyl-6-(thiophen-2-yl)thieno[2,3-b]pyridine-2-carboxamide (9q). Yellow solid; Yield 59% (two steps); ^1H NMR (400 MHz, $\text{DMSO-}d_6$) δ 8.45 (d, $J = 8.5$ Hz, 1H), 7.99 (d, $J = 8.5$ Hz, 1H), 7.93 (d, $J = 3.2$ Hz, 1H), 7.79 (t, $J = 5.5$ Hz, 1H), 7.71 (d, $J = 4.9$ Hz, 1H), 7.33–7.16 (m, 8H), 3.49–3.41 (m, 2H), 2.89–2.81 (m, 2H); ^{13}C NMR (126 MHz, $\text{DMSO-}d_6$) δ 164.80, 158.19, 152.07, 145.27, 143.74, 139.55, 131.44, 129.38, 128.65, 128.63 (2C), 128.35 (2C), 126.75, 126.07, 124.93, 114.99, 97.20, 40.69, 35.47; ESI-MS m/z : 380.6 $[\text{M}+\text{H}]^+$; HRMS (ESI) m/z calcd for $\text{C}_{20}\text{H}_{18}\text{N}_3\text{OS}_2^+$ $[\text{M}+\text{H}]^+$: 380.0886; found: 380.0875.

4.1.6.18

3-amino-N,N-dimethyl-6-(thiophen-2-yl)thieno[2,3-b]pyridine-2-carboxamide (10a). Yellow solid; Yield 42% (two steps); ^1H NMR (400 MHz, $\text{DMSO-}d_6$) δ 8.18 (d, $J = 8.2$ Hz, 1H), 7.97 (dd, $J = 3.7$, 1.0 Hz, 1H), 7.83 (dd, $J = 5.0$, 1.0 Hz, 1H), 7.78 (d, $J = 8.2$ Hz, 1H), 7.23 (dd, $J = 5.0$, 3.7 Hz, 1H), 4.33 (s, 2H), 3.18 (s, 3H), 2.88 (s, 3H); ^{13}C NMR (126 MHz, $\text{DMSO-}d_6$) δ 165.82, 158.72, 151.46, 143.86, 142.77, 131.24, 129.25, 128.61, 126.58, 124.62, 114.88, 98.58, 37.17 (2C); ESI-MS m/z : 304.6 $[\text{M}+\text{H}]^+$; HRMS (ESI) m/z calcd for $\text{C}_{14}\text{H}_{14}\text{N}_3\text{OS}_2^+$ $[\text{M}+\text{H}]^+$: 304.0573; found: 304.0576.

4.1.6.19

3-amino-N-(4-methoxyphenyl)-N-methyl-6-(thiophen-2-yl)thieno[2,3-b]pyridine-2-carboxamide (10b). Yellow solid; Yield 64% (two steps); ^1H NMR (400 MHz, $\text{DMSO-}d_6$) δ 8.42 (d, $J = 8.6$ Hz, 1H), 7.92 (d, $J = 8.6$ Hz, 1H), 7.88 (d, $J = 3.9$ Hz, 1H), 7.68 (d,

$J = 4.9$ Hz, 1H), 7.48 (s, 2H), 7.30 (d, $J = 8.8$ Hz, 2H), 7.17 (dd, $J = 4.9, 3.9$ Hz, 1H), 7.02 (d, $J = 8.8$ Hz, 2H), 3.83 (s, 3H), 3.25 (s, 3H); ^{13}C NMR (126 MHz, DMSO- d_6) δ 165.71, 159.66, 159.06, 152.13, 147.92, 143.76, 135.81, 131.31, 130.44 (2C), 129.35, 128.60, 126.71, 123.25, 114.74 (2C), 114.66, 95.81, 55.38, 38.72; ESI-MS m/z : 396.6 $[\text{M}+\text{H}]^+$; HRMS (ESI) m/z calcd for $\text{C}_{20}\text{H}_{18}\text{N}_3\text{O}_2\text{S}_2^+$ $[\text{M}+\text{H}]^+$: 396.0835; found: 396.0833.

4.1.6.20

3-amino-N-methyl-N-(4-nitrophenyl)-6-(thiophen-2-yl)thieno[2,3-b]pyridine-2-carboxamide (10c). Yellow solid; Yield 52% (two steps); ^1H NMR (400 MHz, DMSO- d_6) δ 8.47 (d, $J = 8.6$ Hz, 1H), 8.27 (d, $J = 9.0$ Hz, 2H), 7.97 (d, $J = 8.6$ Hz, 1H), 7.93–7.89 (dd, $J = 3.6, 1.0$ Hz, 1H), 7.74–7.68 (dd, $J = 4.9, 1.0$ Hz, 1H), 7.61 (d, $J = 9.0$ Hz, 2H), 7.49 (s, 2H), 7.18 (dd, $J = 4.9, 3.8$ Hz, 1H), 3.38 (s, 3H); ^{13}C NMR (126 MHz, DMSO- d_6) δ 166.17, 159.49, 152.61, 149.83, 148.34, 145.19, 143.51, 131.77, 129.68, 128.64, 128.02 (2C), 127.02, 124.74 (2C), 123.54, 114.99, 95.98, 37.97; ESI-MS m/z : 411.6 $[\text{M}+\text{H}]^+$; HRMS (ESI) m/z calcd for $\text{C}_{19}\text{H}_{15}\text{N}_4\text{O}_3\text{S}_2^+$ $[\text{M}+\text{H}]^+$: 411.0580; found: 411.0583.

4.1.6.21

3-amino-N-cyclohexyl-N-methyl-6-(thiophen-2-yl)thieno[2,3-b]pyridine-2-carboxamide (10d). Yellow solid; Yield 68% (two steps); ^1H NMR (400 MHz, DMSO- d_6) δ 8.44 (d, $J = 8.6$ Hz, 1H), 8.01 (d, $J = 8.6$ Hz, 1H), 7.93 (d, $J = 3.8$ Hz, 1H), 7.72 (d, $J = 4.9$ Hz, 1H), 7.20 (dd, $J = 4.9, 3.8$ Hz, 1H), 6.64 (s, 2H), 4.26–4.08 (m, 1H), 2.93 (s, 3H), 1.75 (dd, $J = 26.8, 11.9$ Hz, 4H), 1.66–1.50 (m, 3H), 1.39–1.22 (m, 2H), 1.18–1.03 (m, 1H); ^{13}C NMR (126 MHz, DMSO- d_6) δ 165.78, 158.56, 151.56, 143.84, 143.68, 131.20, 129.26, 128.60, 126.59, 124.68, 114.91, 98.32, 55.70, 30.02 (2C), 29.52, 25.34 (2C), 24.91; ESI-MS m/z : 372.6 $[\text{M}+\text{H}]^+$; HRMS (ESI) m/z calcd for $\text{C}_{19}\text{H}_{22}\text{N}_3\text{O}_2\text{S}_2^+$ $[\text{M}+\text{H}]^+$: 372.1199; found: 372.1191.

4.1.6.22

3-amino-N-methyl-N-(piperidin-4-yl)-6-(thiophen-2-yl)thieno[2,3-b]pyridine-2-carboxamide hydrochloride (10e). Yellow solid; Yield 58% (two steps); ^1H NMR (400 MHz, DMSO- d_6) δ 9.16–8.98 (m, 2H), 8.49 (d, $J = 8.5$ Hz, 1H), 8.01 (d, $J = 8.5$ Hz,

1H), 7.95–7.91 (m, 1H), 7.71 (d, $J = 4.9$ Hz, 1H), 7.20 (dd, $J = 4.9, 3.8$ Hz, 1H), 5.19 (brs, 5H), 4.48–4.37 (m, 1H), 3.34 (d, $J = 11.8$ Hz, 2H), 3.07–2.97 (m, 2H), 2.23–2.00 (m, 2H), 1.86 (d, $J = 12.6$ Hz, 2H); ^{13}C NMR (126 MHz, DMSO- d_6) δ 166.14, 158.67, 151.69, 143.82, 143.40, 131.45, 129.40, 128.69, 126.74, 124.70, 114.98, 98.56, 51.06, 42.72 (2C), 30.18, 25.51 (2C); ESI-MS m/z : 373.6 $[\text{M-HCl}+\text{H}]^+$; HRMS (ESI) m/z calcd for $\text{C}_{18}\text{H}_{21}\text{N}_4\text{OS}_2^+$ $[\text{M-HCl}+\text{H}]^+$: 373.1151; found: 373.1164.

4.1.6.23

3-amino-N-benzyl-N-methyl-6-(thiophen-2-yl)thieno[2,3-b]pyridine-2-carboxamide (10f). Yellow solid; Yield 71% (two steps); ^1H NMR (400 MHz, DMSO- d_6) δ 8.47 (d, $J = 8.6$ Hz, 1H), 8.01 (d, $J = 8.6$ Hz, 1H), 7.93 (d, $J = 3.5$ Hz, 1H), 7.71 (d, $J = 5.0$ Hz, 1H), 7.42–7.35 (m, 2H), 7.32–7.27 (m, 3H), 7.20 (dd, $J = 5.0, 3.5$ Hz, 1H), 6.86 (s, 2H), 4.74 (s, 2H), 3.04 (s, 3H); ^{13}C NMR (126 MHz, DMSO- d_6) δ 166.34, 158.67, 151.76, 144.20, 143.79, 137.56, 131.35, 129.36, 128.62, 128.59 (2C), 127.29 (2C), 127.18, 126.68, 124.44, 114.96, 97.34, 52.47, 35.27; ESI-MS m/z : 380.6 $[\text{M}+\text{H}]^+$; HRMS (ESI) m/z calcd for $\text{C}_{20}\text{H}_{18}\text{N}_3\text{OS}_2^+$ $[\text{M}+\text{H}]^+$: 380.0886; found: 380.0892.

4.1.7

2-(2,4-dimethoxy-3-methylphenyl)-7-(thiophen-2-yl)-9-(trifluoromethyl)pyrido[3',2':4,5]thieno[3,2-d]pyrimidin-4(3H)-one (11).

To a mixture of **DMT** (50.5 mg, 0.1 mmol) in THF (2 mL) added 1,2-dichloro-4,5-dicyanobenzoquinone (DDQ, 45.4 mg, 0.2 mmol) at room temperature. The resulting mixture was allowed to warm to 60 °C over 1 h. Once the reaction was completed as indicated by LC-MS, the reaction mixture was concentrated under reduced pressure and MeOH (2 mL) was added to give a suspension liquid. The solid precipitate was collected by filtration, washed with MeOH (2 mL) and dried under reduced pressure to give the desired product as a yellow solid (45.3 mg, 90%). Yellow solid; ^1H NMR (400 MHz, DMSO- d_6) δ 12.47 (s, 1H), 8.46 (s, 1H), 8.29 (dd, $J = 3.8, 0.9$ Hz, 1H), 7.89 (dd, $J = 5.0, 0.9$ Hz, 1H), 7.82 (d, $J = 8.8$ Hz, 1H), 7.29 (dd, $J = 5.0, 3.8$ Hz, 1H), 7.04 (d, $J = 8.8$ Hz, 1H), 3.90 (s, 3H), 3.65 (s, 3H), 2.16 (s, 3H); ESI-MS m/z : 504.6 $[\text{M}+\text{H}]^+$; HRMS (ESI) m/z calcd for $\text{C}_{23}\text{H}_{17}\text{F}_3\text{N}_3\text{O}_3\text{S}_2^+$ $[\text{M}+\text{H}]^+$: 504.0658; found: 504.0671.

4.1.8. *N*-(pyridin-4-yl)-6-(thiophen-2-yl)thieno[2,3-*b*]pyridine-2-carboxamide (**12**).

A solution of **9d** (246 mg, 0.7 mmol) in DMF (3 ml) was added dropwise to a solution of t-BuONO (2.0 equiv) in DMF (3 ml) at 60°C. After stirring for 0.5 h, the reaction mixture was poured into hydrochloric acid (1 N, 20 mL) to give a suspension liquid. The solid precipitate was collected by filtration. To the mixture of the solid precipitate in EtOH (6 mL) was added Zn power (195 mg, 3 mmol) at room temperature. The resulting mixture was allowed to warm to 100 °C. Once the reaction was completed as indicated by LC-MS, the reaction mixture was concentrated under reduced pressure. The appropriate compound was obtained following purification by silica gel column chromatography. Yellow solid; Yield 73% (two steps); ¹H NMR (400 MHz, DMSO-*d*₆) δ 10.91 (s, 1H), 8.52 (dd, *J* = 4.9, 1.4 Hz, 2H), 8.48 (d, *J* = 8.5 Hz, 1H), 8.39 (s, 1H), 8.10 (d, *J* = 8.5 Hz, 1H), 8.00 (dd, *J* = 3.8, 1.0 Hz, 1H), 7.81–7.75 (m, 3H), 7.23 (dd, *J* = 4.9, 3.8 Hz, 1H); ¹³C NMR (126 MHz, DMSO-*d*₆) δ 161.57, 160.85, 151.49, 150.46 (2C), 145.30, 143.59, 137.80, 134.53, 131.23, 129.86, 128.76, 127.22, 125.11, 116.60, 113.97 (2C); ESI-MS *m/z*: 338.6 [M+H]⁺; HRMS (ESI) *m/z* calcd for C₁₇H₁₂N₃OS₂⁺ [M+H]⁺: 338.0416; found: 338.0411.

4.2 Biological evaluation

4.2.1. Hepatic glucose output assay

HGP assay was conducted according to the previous study with modification (Zhang, et al. 2013). In the assay, freshly isolated mouse hepatocytes were seeded onto 48-well plates with standard Williams' E medium. After 4-h attachment, cells were changed to serum-free minimum essential medium (MEM) and incubated with corresponding compounds and 10 nM glucagon for 16 h. After washing with PBS twice to remove the remaining glucose, cells were incubated with compounds and 10nM glucagon in 500 μL glucose production detection buffer (glucose-free DMEM without phenol red containing 20 mM sodium lactate and 2 mM sodium pyruvate). After 6-h incubation, 50 μL detection buffer was collected for glucose concentration measurement with a colorimetric glucose assay kit (Nanjing Jiancheng, Nanjing, China) according to the manufacturer's instruction. The results were normalized to the total protein concentration measured by BCA protein kit (Thermo Scientific, MA,

USA).

4.2.2. The mRNA levels of G6Pase and PEPCK Assay

Primary hepatocytes were seeded onto 6-well plates. After 4-h attachment, cells were replaced to MEM supplemented with 10% FBS, 100 U/mL penicillin and 100 mg/mL streptomycin. Cells were incubated with corresponding compounds for 24 h and stimulated with 10 nM glucagon together for another 2 h. Total RNA from cultured mouse hepatocytes or mashed liver tissues was extracted using TRIzol reagent according to the manufacturer's protocol (Takara Bio Inc, Dalian, China). Complementary DNAs were generated by PrimeScript™ RT reagent Kit (Takara Bio Inc, Dalian, China) and analyzed qPCR assay using SYBR® Premix Ex Taq™ (Takara Bio Inc, Dalian, China) on a Bio-Rad CFX Connect™ Real-Time System (Bio-Rad Company, CA, USA). The mRNA levels of specific genes were normalized to GAPDH. The primers for qPCR were generated from Sangon Biotech (Shanghai, China) as follows:

G6Pase (+), TAATTGGCTCTGCCAATGGCGATC;

G6Pase (-), ATCAGTCTGTGCCTTGCCCCTGT;

PEPCK (+), CTGCATAACGGTCTGGACTTC;

PEPCK (-), CAGCAACTGCCCCGTACTCC;

GAPDH (+), ACAGCAACAGGGTGGTGGAC;

GAPDH (-), TTTGAGGGTGCAGCGAACTT.

4.2.3. In vivo assay

All animals were received humane care, and animal-related protocols were approved by the Institutional Animal Care and Use Committees at Shanghai Institute of Materia Medica, Chinese Academy of Sciences. *db/db* mice (BKS.Cg-*Dock7*^{m+/+}*Lepr*^{db/J}) were from Jackson Laboratory (CA, USA). 8-week-old mice were divided into 2 groups by fasting blood glucose and body weight. Vehicle or **8e** (25 mg/Kg) was administrated by intraperitoneal injection daily for 5 weeks. Fasting blood glucose levels from 6-h fasted mice were measured weekly. At the termination of the assay, mice were sacrificed and liver tissues were stored at -80 °C for analysis.

Oral glucose tolerance test (OGTT) - For the glucose tolerance test, the mice were

fasted for 16 h at the fourth week, 1.5 g/Kg glucose was administered orally with a gavage needle. Glucose levels were measured from tail vein blood samples at 0, 15, 30, 60, 90 and 120 min by ACCU-CHEK active blood sugar system (Roche, Basel, Switzerland).

Pyruvate tolerance test (PTT) - For the pyruvate tolerance test, the mice were fasted for 16 h at the fifth week and then injected intraperitoneally with sodium pyruvate (1.5 g/Kg). Blood glucose levels were measured with tail vein blood samples at 0, 15, 30, 60, 90 and 120 min.

Acknowledgements

This work was supported by the National Natural Science Foundation of China (grants 81473110, 81773596, 81561148011, 8170130685), Natural Science Foundation of Jiangsu Higher Education Institutions (grant: 17KJA360004, 16KJB350003), Natural Science Foundation of Jiangsu (grants SBK2016043296), Program of Outstanding Scientific and Technological Innovation Team of Jiangsu Higher Education Institutions, and the Priority Academic Program Development of Jiangsu Higher Education Institutions.

Reference

- [1] L. Guariguata, D.R. Whiting, I. Hambleton, J. Beagley, U. Linnenkamp, J.E. Shaw, *Diabetes Res. Clin. Pract.* 103 (2014) 137-149.
- [2] A. Dwarakanathan, *J Insur Med* 38 (2006) 20-30.
- [3] X. Xu, G. Wang, T. Zhou, L. Chen, J. Chen, X. Shen, *Expert Opinion on Drug Discovery* 9 (2014) 1047-1058.
- [4] G. Brown, A. Singer, V.V. Lunin, M. Proudfoot, T. Skarina, R. Flick, S. Kochinyan, R. Sanishvili, A. Joachimiak, A.M. Edwards, A. Savchenko, A.F. Yakunin, *Journal of Biological Chemistry* 284 (2009) 3784-3792.
- [5] S. Jitrapakdee, *The International Journal of Biochemistry & Cell Biology* 44 (2012) 33-45.
- [6] Y.-Y. Wang, C.-J. Chen, S.-Y. Lin, Y.-H. Chuang, W.H.-H. Sheu, K.-C. Tung, *Molecular and Cellular Endocrinology* 367 (2013) 50-56.
- [7] G. Jiang, B.B. Zhang, *American Journal of Physiology - Endocrinology And Metabolism* 284 (2003) E671-E678.
- [8] Y. Liu, R. Dentin, D. Chen, S. Hedrick, K. Ravnskjaer, S. Schenk, J. Milne, D.J. Meyers, P. Cole, J.Y. Iii, J. Olefsky, L. Guarente, M. Montminy, *Nature* 456 (2008) 269-273.
- [9] Y. Wang, G. Li, J. Goode, J.C. Paz, K. Ouyang, R. Sreaton, W.H. Fischer, J. Chen, I. Tabas, M. Montminy, *Nature* 485 (2012) 128-132.
- [10] L. Rui, *Energy Metabolism in the Liver*. In *Comprehensive Physiology*, John Wiley & Sons, Inc.: 2014; Vol. 4, pp 177-197.

- [11] R. Dentin, Y. Liu, S.-H. Koo, S. Hedrick, T. Vargas, J. Heredia, J. Yates, M. Montminy, *Nature* 449 (2007) 366-369.
- [12] L. He, A. Sabet, S. Djedjos, R. Miller, X. Sun, M.A. Hussain, S. Radovick, F.E. Wondisford, *Cell* 137 (2009) 635-646.
- [13] A. Barthel, D. Schmolz, *American Journal of Physiology - Endocrinology And Metabolism* 285 (2003) E685-E692.
- [14] D. Granner, T. Andreone, K. Sasaki, E. Beale, *Nature* 305 (1983) 549-551.
- [15] A.K. Rines, K. Sharabi, C.D.J. Tavares, P. Puigserver, *Nat Rev Drug Discov* 15 (2016) 786-804.
- [16] A.K. Madiraju, D.M. Erion, Y. Rahimi, X.-M. Zhang, D.T. Braddock, R.A. Albright, B.J. Prigaro, J.L. Wood, S. Bhanot, M.J. MacDonald, M.J. Jurczak, J.-P. Camporez, H.-Y. Lee, G.W. Cline, V.T. Samuel, R.G. Kibbey, G.I. Shulman, *Nature* 510 (2014) 542-546.
- [17] R.A. DeFronzo, R.E. Ratner, J. Han, D.D. Kim, M.S. Fineman, A.D. Baron, *Diabetes Care* 28 (2005) 1092-1100.
- [18] J. Rosenstock, R. Brazg, P.J. Andryuk, K. Lu, P. Stein, *Clinical Therapeutics* 28 (2006) 1556-1568.
- [19] F.X. Pi-Sunyer, A. Schweizer, D. Mills, S. Dejager, *Diabetes Res. Clin. Pract.* 76 (2007) 132-138.
- [20] W. Meng, B.A. Ellsworth, A.A. Nirschl, P.J. McCann, M. Patel, R.N. Girotra, G. Wu, P.M. Sher, E.P. Morrison, S.A. Biller, R. Zahler, P.P. Deshpande, A. Pullockaran, D.L. Hagan, N. Morgan, J.R. Taylor, M.T. Obermeier, W.G. Humphreys, A. Khanna, L. Discenza, J.G. Robertson, A. Wang, S. Han, J.R. Wetterau, E.B. Janovitz, O.P. Flint, J.M. Whaley, W.N. Washburn, *Journal of Medicinal Chemistry* 51 (2008) 1145-1149.
- [21] S. Nomura, S. Sakamaki, M. Hongu, E. Kawanishi, Y. Koga, T. Sakamoto, Y. Yamamoto, K. Ueta, H. Kimata, K. Nakayama, M. Tsuda-Tsukimoto, *Journal of Medicinal Chemistry* 53 (2010) 6355-6360.
- [22] J.C. Yoon, P. Puigserver, G. Chen, J. Donovan, Z. Wu, J. Rhee, G. Adelmant, J. Stafford, C.R. Kahn, D.K. Granner, C.B. Newgard, B.M. Spiegelman, *Nature* 413 (2001) 131-138.
- [23] H. An, L. He, *Journal of Endocrinology* 228 (2016) R97-R106.
- [24] Y.-S. Yoon, D. Ryu, M.-W. Lee, S. Hong, S.-H. Koo, *Exp Mol Med* 41 (2009) 577-583.
- [25] T.T. Zhou, F. Ma, X.F. Shi, X. Xu, T. Du, X.D. Guo, G.H. Wang, L. Yu, V. Rukachaisirikul, L.H. Hu, J. Chen, X. Shen, *Journal of Molecular Endocrinology* 59 (2017) 151-169.

Captions:

Figure 1. The structure of **DMT** and the four regions SARs study focused on

Figure 2. **8e** inhibited hepatic gluconeogenic genes G6Pase and PEPCK in dose-dependent manner

Figure 3. **8e** ameliorated hyperglycemia in *db/db* mice in dose-dependent manner

Scheme 1. Reagents and conditions

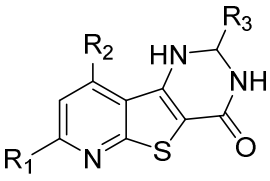
Scheme 2. Synthetic route of compound **11**

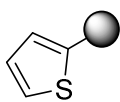
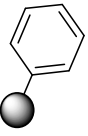
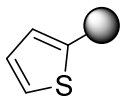
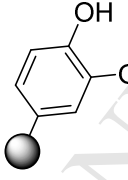
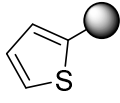
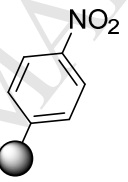
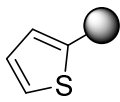
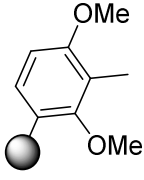
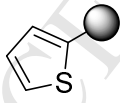
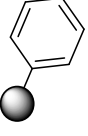
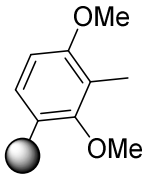
Scheme 3. Synthetic route of compound **12**

Table 1. Inhibition of hepatic glucose production activities with **8a-8f**

Table 2. Inhibition of hepatic glucose production activities with **9a-9q** and **12**

Table 3. Inhibition of hepatic glucose production activities with **10a-10f**

Table 1. Inhibition of hepatic glucose production activities with **8a-8f**


Compd.	R ₁	R ₂	R ₃	IC ₅₀ (μM) ^a	cLog P ^b
DMT				33.9	4.714
8a		CF ₃		24.8	4.246
8b		CF ₃		30.2	3.735
8c		CF ₃		1.7	3.756
8d		H		15.4	4.127
8e		H		16.8	2.986
8f	CH ₃	CF ₃		NA	3.661

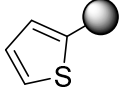
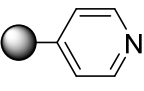
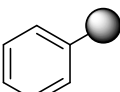
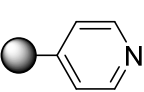
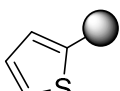
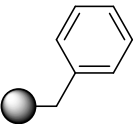
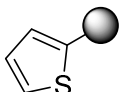
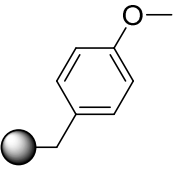
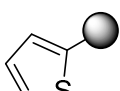
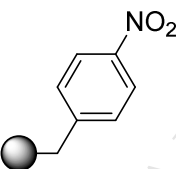
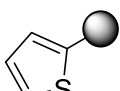
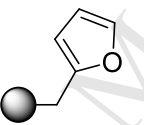
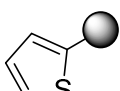
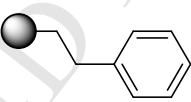
^aIC₅₀: 50% inhibitory concentration. The biological data are generated from at least three independent experiments.

^b: The cLog P values were calculated by ACD-Labs (Version 6.0).

NA: compound showing IC₅₀ value > 100 μM.

Table 2. Inhibition of hepatic glucose production activities with **9a-9q** and **12**

Compd.	R ₁	R ₂	R ₄	IC ₅₀ (μM) ^a	cLog P ^b
DMT				33.9	4.714
9a		H		12.3	3.661
9b		H		19.1	3.744
9c		H		33.4	3.800
9d		H		12.3	2.858
9e		H		24.7	3.066
9f		H		14.6	4.928
9g		H		NA	3.266
9h		H		NA	3.931
9i		H		14.2	2.715
			NH ⁺ •HCl		
9j		H		8.0	3.490

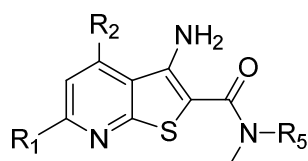
9k		CH ₃		NA	3.187
9l		H		14.4	3.234
9m		H		12.4	4.132
9n		H		10.3	4.198
9o		H		34.1	3.450
9p		H		54.0	3.388
9q		H		NA	4.514
12				65.3	3.878

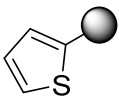
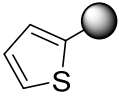
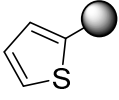
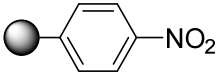
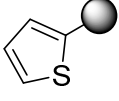
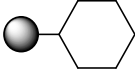
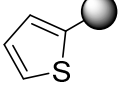
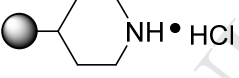
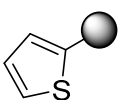
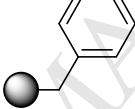
^aIC₅₀: 50% inhibitory concentration. The biological data are generated from at least three independent experiments.

^b: The cLog P values were calculated by ACD-Labs (Version 6.0).

NA: compound showing IC₅₀ value > 100 μM.

Table 3. Inhibition of hepatic glucose production activities with **10a-10f**



Compd.	R ₁	R ₂	R ₅	IC ₅₀ (μM) ^a	cLog P ^b
DMT				33.9	4.714
10a		H	CH ₃	NA	3.224
10b		H		26.3	3.882
10c		H		37.8	3.129
10d		H		NA	4.073
10e		H		22.1	2.782
10f		H		17.8	4.452

^aIC₅₀: 50% inhibitory concentration. The biological data are generated from at least three independent experiments.

^b: The cLog P values were calculated by ACD-Labs (Version 6.0).

NA: compound showing IC₅₀ value > 100 μM.

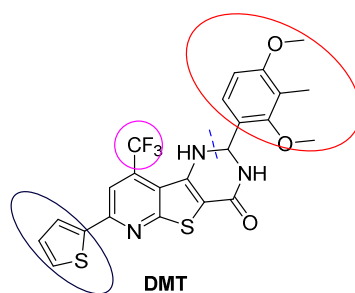


Figure 1. The structure of **DMT** and the four regions SARs study focused on

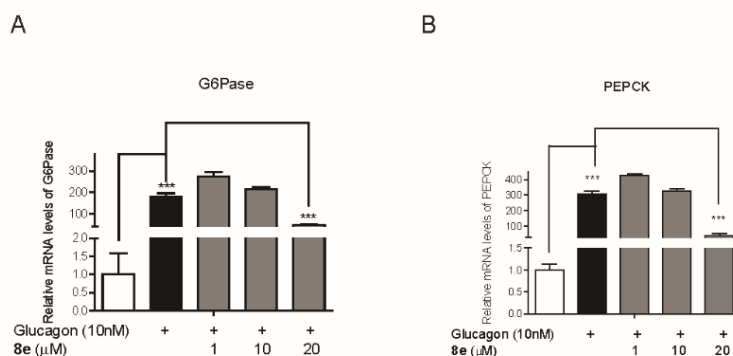


Figure 2. **8e** inhibited hepatic gluconeogenic genes G6Pase in dose-dependent manner (A) and PEPCK (B). All data were obtained from three independent experiments and presented as means \pm SEM (** p <0.01, *** p <0.001).

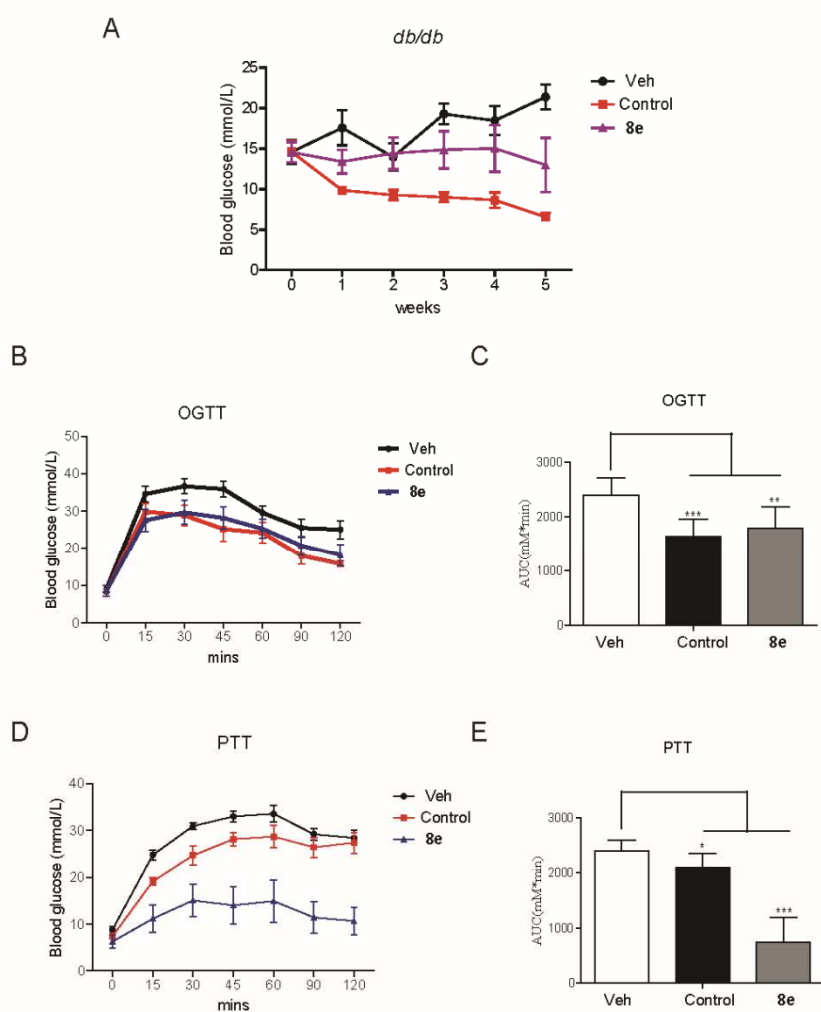
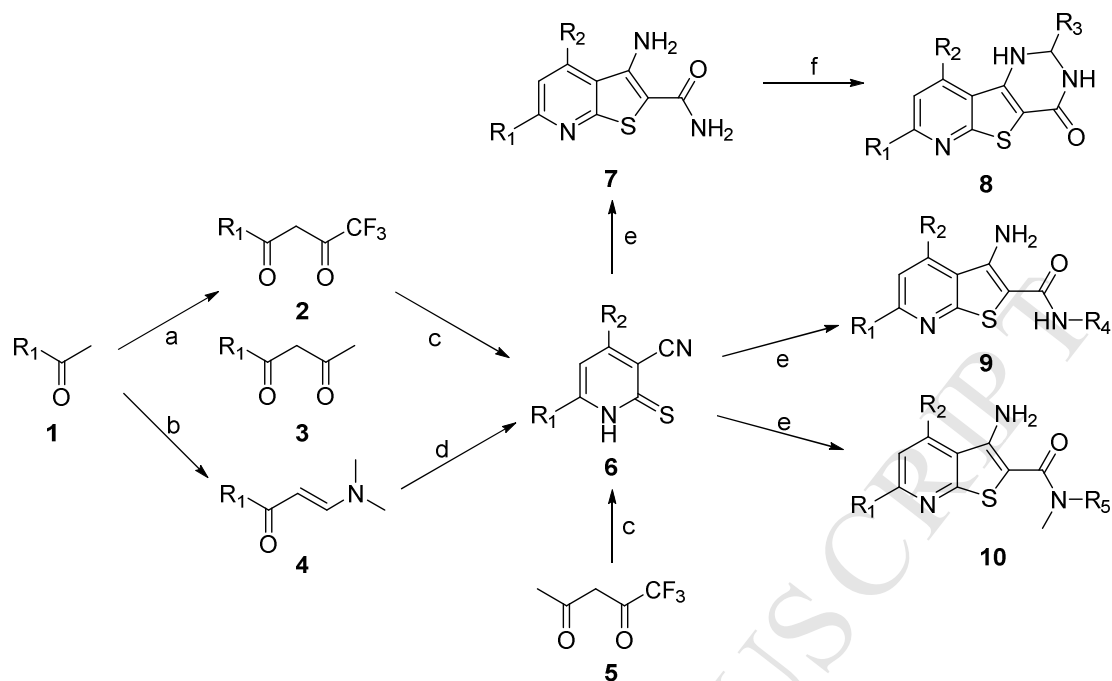
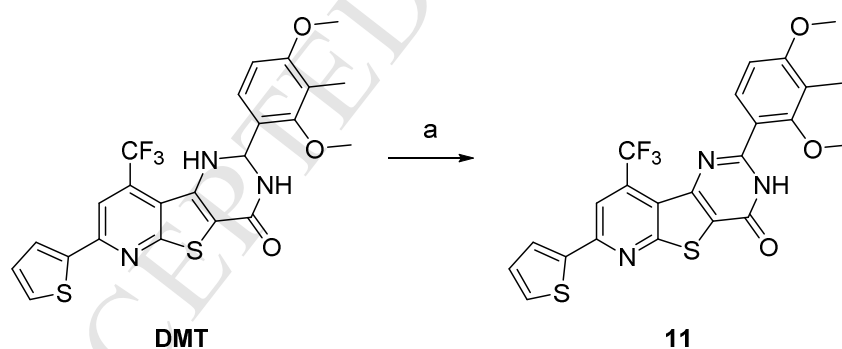


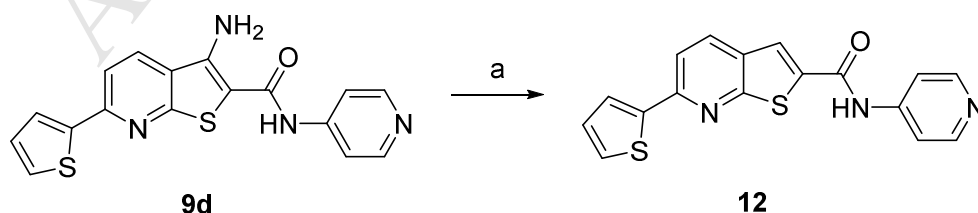
Figure 3. 8e ameliorated hyperglycemia in *db/db* mice in dose-dependent manner. (A). Fasting blood glucose levels were detected weekly in *db/db* mice with treatment of 8e (25 mg/Kg/day) (n=8) and Rosiglitazone (10 mg/Kg/day) (n=8); (B & C). OGTT assay was performed in *db/db* mice after treatment with 8e (25 mg/Kg/day) and Rosiglitazone (10 mg/Kg/day) for 4 weeks (n=8); (D & E) PTT assay was performed in *db/db* mice after treatment with 8e (25 mg/Kg/day) and Rosiglitazone (10 mg/Kg/day) for 5 weeks (n=8). All data were presented as means \pm SEM (*p<0.05, **p<0.01).



Scheme 1. Reagents and conditions: (a) ethyl trifluoroacetate (for **3**) or ethyl acetate (for **4**), potassium tert-butoxide, toluene, 0 °C–rt; (b) DMF-DMA, DMF, 80 °C; (c) cyanothioacetamide, triethylamine, ethanol, 80 °C; (d) cyanothioacetamide, DABCO, ethanol, 80 °C; (e) DMF, KOH (10%), 2-chloro-acetamid (for **7**), chloroacetamides (for **9** and **10**); (f) aldehydes, AcOH, reflux.



Scheme 2. Synthesis routine of compound **11**: (a) DDQ, THF, 60 °C.



Scheme 3. Synthesis routine of compound **12**: (a) tert-butyl nitrite, DMF, 80 °C.

Highlights

- (1). Regulation of gluconeogenesis could regulate blood glucose levels in T2DM.
- (2). Several DMT derivatives were designed and synthesized.
- (3). Systematic SAR investigation of **DMT** derivatives.
- (4). **8e** exhibited more potent biological activity in vitro and in vivo.